© Indian Academy of Sciences

Characterisation of particulate matter at a high-altitude site in southwest India: Impact of dust episodes

P Buchunde[1,2], P D Safai[1,*], S Mukherjee[1], P P Leena[1], D Siingh[1],
G S Meena[1] and G Pandithurai[1]

[1]*Indian Institute of Tropical Meteorology, Pune 411 008, India.*
[2]*Department of Atmospheric and Space Sciences, Savitribai Phule, Pune University, Pune, India.*
Corresponding author. e-mail: pdsafai@tropmet.res.in

Observations on a particulate matter (PM_{10} and $PM_{2.5}$) were carried out during March 2015 to February 2017 over a high-altitude location Mahabaleshwar in the Western Ghats region in southwest India. Apart from temporal variation of PM and the ratio of $PM_{2.5}/PM_{10}$, impacts of local meteorological parameters on the concentration of PM are examined. PM_{10} showed a maximum concentration during pre-monsoon, whereas $PM_{2.5}$ showed it in winter. The monsoon season showed the lowest concentrations for both PM_{10} and $PM_{2.5}$. Concentrations were significantly reduced in 2016 due to the washout effect from enhanced rainfall during that year. Diurnal variations of PM were related to the variation in a planetary boundary layer, mountain valley winds as well as changes in different local sources. Dominance of primary particles was observed from the $PM_{2.5}/PM_{10}$ ratio. The Central Pollution Control Board (CPCB) threshold limit for PM was exceeded on several days mainly during pre-monsoon due to transported dust from the Arabian Peninsula and Thar Desert apart from an increase in the tourist activity. A typical case for transported dust event during March 2016 is studied. Organics and sulphate particles showed a significant enhancement during dust event. Overall, the study indicated emissions from mixed sources for PM from local as well as distant source regions over Mahabaleshwar.

Keywords. $PM_{2.5}$ and PM_{10}; diurnal and seasonal variation; meteorological parameters; dust event; long-range transport; concentration weighted trajectories.

1. Introduction

Characterisation of atmospheric aerosols which are also termed as particulate matter (PM) poses a great challenge due to their variation in terms of spatial and temporal scales. Primary aerosols are directly injected into the atmosphere, while secondary ones are generated from gas-to-particle conversion mechanisms (Khemani 1989; Safai *et al.* 2010). PM constitutes one of the most challenging problems in terms of both air quality and climate change policies. Sources of PM include all types of combustion, such as emission from motor vehicles, power plants, residential wood burning, forest fires, agricultural burning, industrial processes and construction and demolition activities. Aerosols play a major role in several atmospheric phenomena such as air pollution, acid deposition, visibility degradation, radiation balance, precipitation formation, etc. (Khemani 1989). PM is one of the major urban air pollutants and it has been related to cardiovascular diseases and strokes (Burnett *et al.* 2014; Du *et al.* 2016), respiratory disorders, pulmonary diseases (Song *et al.* 2014) and even cognitive

problems (Weuve *et al.* 2012). It has also been associated with millions of premature deaths annually (WHO 2016). Size and chemical composition of PM are the important factors affecting the air quality at any location. Transport of $PM_{2.5}$ from regional and/or distant sources also contributes to the local air quality (van Donkelaar *et al.* 2010). From the health point of view, penetration of particles into the respiratory tract is a function of the particle size and the ratio of $PM_{2.5}/PM_{10}$ is very critical. The high $PM_{2.5}/PM_{10}$ ratio attributes emission from combustion activities and the formation of secondary pollutants in the atmosphere. On the other hand, low $PM_{2.5}/PM_{10}$ ratios are related to more contribution from primary sources such as influx of dust or sea salt.

So far studies on fine sized PM ($PM_{2.5,}$ i.e., PM ≤ 2.5 µm) and coarse sized PM ($PM_{10,}$ i.e., PM ≤ 10 µm) are reported mainly for urban locations in India (Rengarajan *et al.* 2011; Tiwari *et al.* 2012, 2013; Panicker *et al.* 2015; Pipal and Satsangi 2015; Gawhane *et al.* 2017). Very few studies are reported from high-altitude stations in India (Safai *et al.* 2005; Chatterjee *et al.* 2010; Satsangi *et al.* 2014; Leena *et al.* 2017). Satsangi *et al.* (2014) have reported mean concentration of PM_{10} (35.8 $\pm$ 15.2 µg m^{-3}) and $PM_{2.5}$ (14.1 $\pm$ 8.2 µg m^{-3}) at Sinhagad (1450 m above mean sea level (AMSL), a rural high-altitude location in the Western Ghats mountainous region during November 2008 to April 2009. Chatterjee *et al.* (2010) reported $PM_{2.5}$ and PM_{10} over Darjeeling (2200 m AMSL), a high-altitude site in Eastern Himalayan ranges during January–December 2005. They reported $PM_{2.5}$ dominated during dry seasons and PM_{10} dominated during monsoon. Similarly, a long-range transport of dust aerosol from arid regions of Western India was observed during pre-monsoon. Leena *et al.* (2017) have reported variation of PM at Mahabaleshwar during 2012–2013 and its relationship with gaseous pollutants as well as prevailing meteorological parameters. The present paper examines the temporal variation of $PM_{2.5}$ and PM_{10} at Mahabaleshwar during March 2015–March 2017. Exceedances of Central Pollution Control Board (CPCB) threshold limits for PM_{10} and $PM_{2.5}$ are reported. Diurnal and seasonal variations of weather-related parameters such as temperature, wind direction (WD), wind speed (WS) and humidity and their impact on variation of PM are also studied. The possible long-range transport of PM is examined using air mass back trajectories for different seasons. In addition to it, observations of omega winds, concentration weighted trajectories (CWTs) and NCEP winds have been used to ascertain the source regions during the dust event day.

2. Sampling location, meteorology and methodology

2.1 *Sampling location*

Mahabaleshwar (17.92°N, 73.65°E, 1348 m AMSL) is a beautiful hill station surrounded by forests in the midst of Sahyadri mountain ranges in the Western Ghats region in southwest India. It is 120 km south of Pune which is one of the important urban centres in India. Observations were conducted at the High Altitude Cloud Physics Laboratory (HACPL) at Mahabaleshwar. Figure 1 shows the location of Mahabaleshwar on the map of India and the sampling site in the inset. The site is also a popular weekend gateway especially more during pre-monsoon. Figure 2 shows the number of visitors and vehicles visiting Mahabaleshwar since 2007–2016 annually. Vehicular and visitor count data during this period over Mahabaleshwar were obtained from the Nagar Parishad, Mahabaleshwar which shows a linear increase in both visitors and vehicles in the last one decade. Nearly 1 million tourists and 0.12 million vehicles visited Mahabaleshwar in 2007 whereas in 2016, about 2 million tourists and 0.33 million vehicles visited the hill station. The pre-monsoon season, especially during weekends recorded highest tourist influx.

2.2 *Local meteorology*

During the study period, meteorological data for major parameters such as temperature, relative humidity (RH), WS and direction and rainfall were obtained using an automatic weather station (AWS) at a sampling rate of 1 min. The statistical details of the observed meteorological parameters are shown in table 1. To describe the seasonal trends, the PM_{10} and $PM_{2.5}$ mass concentrations were categorised into pre-monsoon (March–May), Monsoon (June–September), post-monsoon (October–November) and winter (December–February). During pre-monsoon, north-westerly winds were dominant, whereas westerly/north-westerly winds mainly prevailed during monsoon. South-easterly winds were dominant during post-monsoon and winter seasons.
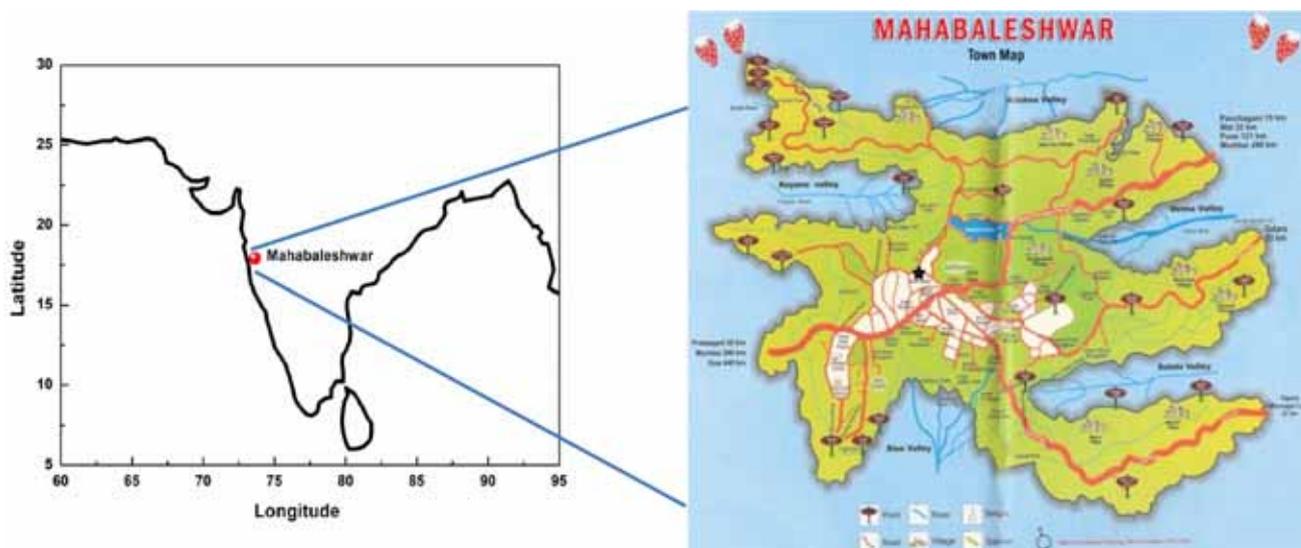
Figure 1. Location of Mahabaleshwar on the map of India and the sampling site in the inset.
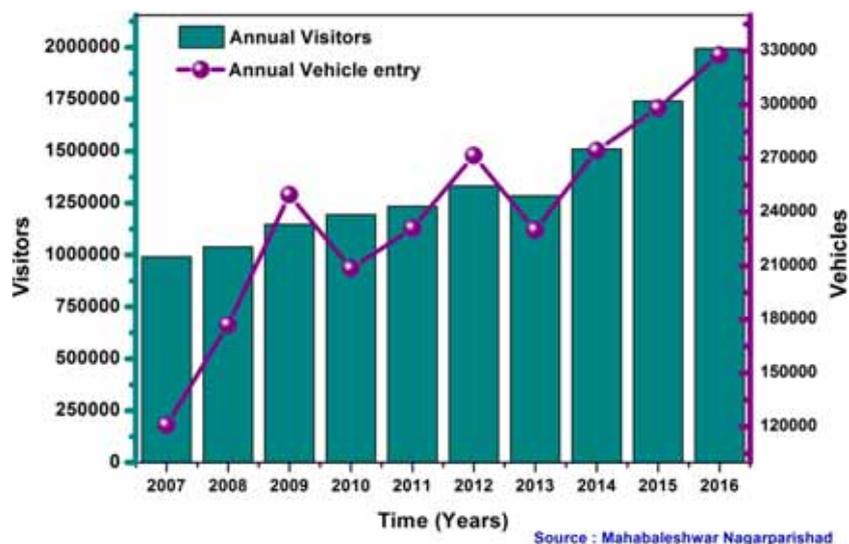

Figure 2. Annual number of visitors and vehicles that visited Mahabaleshwar during 2007 to 2016.

2.3 *Methodology*

Measurements on mass concentration of airborne PM were carried out using GRIMM Environmental Dust Monitor (EDM 180) from GRIMM Aerosol Technik, Germany. The operating principle of this equipment involves measurement of scattering of laser beam at a wavelength of 655 nm by particles passing through it. After amplification, the scattered light at 90° is passed through a diode and then categorised into different sized channels. The EDM measures between 0.25 and 32 μm diameters in discrete 31 channels. The reproducibility varies ± 3% of the total measuring range and it is online calibrated with a in-built temperature and humidity sensor for air density flow rate calculation. The sample flow rate of 1.2 l/min, ±3% constant due self-regulation is maintained and data are obtained at every 5 min interval. The equipment has an isothermal inlet with an integrated Nafion dryer that allows the use of a dehumidification system above 70% RH to remove humidity from the sample pipe to get rid of any condensation during the measurement. Gravimetric and optical calibration of the equipment is performed every year. A study conducted by the Stockholm University, Sweden for the Swedish Environmental Protection Agency during 2012 has reported that

Table 1. *Statistical details of the meteorological parameters during the period of observations at Mahabaleshwar.*

Parameter	Pre-monsoon		Monsoon		Post-monsoon		Winter	
	2015	2016	2015	2016	2015	2016	2016	2017
Temperature: °C								
Mean (SD)	25.10 (0.67)	25.31 (1.35)	19.89 (1.44)	19.21 (1.0)	21.37 (1.0)	19.21 (1.0)	20.77 (2.61)	20.92 (1.37)
Maximum	25.86	26.34	21.88	20.23	20.65	20.23	18.37	21.89
Minimum	24.23	23.77	15.56	18.06	22.09	18.06	23.57	19.95
RH: %								
Mean (SD)	92.98 (8.90)	95.67 (1.45)	92.98 (8.90)	95.67 (1.45)	68.17 (5.83)	65.75 (13.7)	43.72 (9.14)	52.6 (18.7)
Maximum	99.76	97.09	99.76	97.09	72.30	75.47	52.63	97.7
Minimum	81.11	93.75	81.11	93.75	64.05	56.05	34.36	10.2
Wind speed: m s^{-1}								
Mean (SD)	3.10 (0.47)	2.84 (0.19)	3.36 (1.02)	3.50 (0.70)	3.95 (1.09)	3.31 (0.87)	2.94 (0.81)	3.65 (0.87)
Maximum	3.56	3.06	4.87	4.35	3.18	3.94	3.85	4.62
Minimum	2.56	2.682	2.70	2.65	4.71	2.69	2.29	2.92
Total rainfall: mm	194	38.5	3776	6735	173	176.5	10	7

results from Grimm EDM 180 evaluated against the reference sampler equipped with an US-EPA inlet showed <20% uncertainty (ACES 2012).

During a particular dust event in pre-monsoon, the mass spectra of non-refractory submicron PM (NR PM$_1$) were recorded using a time of flight aerosol chemical speciation monitor (ToF-ACSM). The chemical speciation of NR PM$_1$ which vaporises at about 600°C and 10^{-7} mbar was achieved by analysis of fragmentation patterns (Allan *et al.* 2004). More details on this instrument are discussed elsewhere (Ng *et al.* 2011; Frohlich *et al.* 2013; Singla *et al.* 2017).

An AWS was used to monitor the meteorological conditions prevailing over the observational site such as WD, WS, temperature (T), RH and rainfall (R). Also we have used a National Oceanic and Atmospheric Administration (NOAA) Hybrid Single Particle Lagrangian Integrated Trajectory (HYSPLIT) model (Draxler and Rolph 2003) to obtain air-mass back trajectories. These back trajectories were used to infer the possible distant sources of the PM.

3. Results and discussion

3.1 *Monthly variation of PM and PM$_{2.5}$/PM$_{10}$ ratio*

Figure 3 depicts the mean monthly mass concentration of PM$_{10}$ and PM$_{2.5}$ during the entire study period along with the ratio of PM$_{2.5}$ to PM$_{10}$. Analysis of PM data showed that in 2015, the maximum concentration for PM$_{10}$ (81.37 ± 17.43 µg m^{-3}) was observed in April and that for PM$_{2.5}$ (48.49 ± 9.58 µg m^{-3}) was observed in March. In the year 2016, the highest concentration for PM$_{10}$ was observed in March (62.92 ± 26.12 µg m^{-3}), whereas for PM$_{2.5}$ (46.86 ± 16.82 µg m^{-3}) it was observed in February. The minimum concentration was observed in August of 2016 with 2.87 ± 1.39 µg m^{-3} for PM$_{10}$ and 2.85 ± 1.38 µg m^{-3} for PM$_{2.5}$. In 2015, the minimum was observed in the month of July with 5.96 ± 3.88 µg m^3 for PM$_{10}$ and 4.86 ± 2.46 µg m^{-3} for PM$_{2.5}$. Concentrations of both PM$_{10}$ and PM$_{2.5}$ showed a decrease in 2016 than those in 2015. As seen from figure 2, the number of visitors and vehicles increased in 2016 than those in 2015 which should have resulted in an increase in PM load. However, there seems to be a competing effect of more rainfall scavenging that countered and overcame the increase in the anthropogenic source of PM in terms of visitors and vehicles resulting in a net decrease in PM load over the study location during 2016.

The observed concentrations of PM$_{10}$ and PM$_{2.5}$ at Mahabaleshwar are compared with those reported for other similar sites in India and elsewhere (table 2). It is seen that PM$_{10}$ concentrations at Mahabaleshwar were comparable with those reported at some other high-altitude locations like Lhasa, Sinhagad and Darjeeling, whereas PM$_{2.5}$ was more at Mahabaleshwar than that reported at these locations. However, PM$_{10}$ and PM$_{2.5}$ concentrations at Mahabaleshwar were comparatively less than those reported at Kathmandu, Nepal which is almost at the same altitude like Mahabaleshwar. Also, concentrations of PM$_{10}$
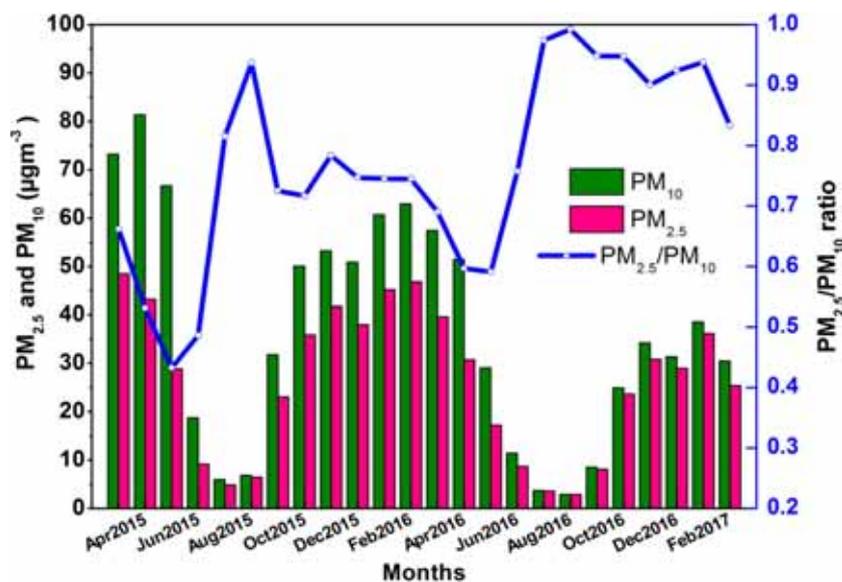
Figure 3. Mean monthly mass concentration of PM_{10} and $PM_{2.5}$ during March 2015 to February 2017 along with the ratio of $PM_{2.5}$ to PM_{10}.

and $PM_{2.5}$ were much higher at other urban locations than those observed at Mahabaleshwar which is quite expected. Sreekanth *et al.* (2018) have reported $PM_{2.5}$ concentrations over five metro cities in India. They have reported the annual mean ($\pm$ standard deviation) concentrations of $PM_{2.5}$ as 37 ± 17, 51 ± 23, 54 ± 36, 80 ± 67 and 114 ± 86 μg m^{-3} over Chennai, Hyderabad, Mumbai, Kolkata and Delhi, respectively. The annual mean $PM_{2.5}$ concentration at Mahabaleshwar during 2015–2016 (31 ± 16.3 μg m^{-3}) and 2016–2017 (21.3 ± 12.9 μg m^{-3}) is found to be comparatively less than the above-mentioned values for five metro cities in India. Carrico *et al.* (2003) studied the PM over the Kathmandu valley, Nepal (Nagarkot 2150 m AMSL) from December 1998 through October 2000 and found higher $PM_{2.5}$ (59 ± 61 μg m^{-3}) in February to May and lower during June to September with a steady increase during October to January (25 ± 14 μg m^{-3}). They have also suggested the possible effect of long-range transport of desert dust to the Himalaya from arid regions ranging from India and the Middle East or even from the Sahara along with the Kathmandu valley effect.

Generation and composition of PM_{10} and $PM_{2.5}$ are decided by various source activities. The ratio of the mass concentration of PM_{10} and $PM_{2.5}$ ($PM_{2.5}/PM_{10}$) indicates the contribution from natural and anthropogenic sources (Querol *et al.* 2004). The low $PM_{2.5}/PM_{10}$ mass ratio infers to the dominance of primary or natural sources such as

soil dust, sea salt, etc. (Chan and Yao 2008) whereas, the higher ratio shows more contribution from secondary particles originated from combustion activities (Perez *et al.* 2008). In the present study, pre-monsoon showed the lowest $PM_{2.5}/PM_{10}$ ratio (0.54 in 2015 and 0.61 in 2016). This ratio in monsoon was 0.74 and 0.91 in 2015 and 2016, respectively. In post-monsoon it was 0.75 and 0.92 in 2015 and 2016, respectively, whereas in winter it was 0.74 and 0.90 in 2016 and 2017, respectively. This confirms the major role of primary sources especially, dust particles. The coarse particles associated with the Asian dust storms have been reported to be the major pollutants in pre-monsoon (Wang *et al.* 2011). The average ratio of $PM_{2.5}/PM_{10}$ for 2015–2016 was 0.69 and that for 2016–2017 was 0.84 at Mahabaleshwar indicating the dominance of primary particle emissions by natural and man-made activities. The $PM_{2.5}/PM_{10}$ ratio was reported to be 0.37 at Lhasa, the capital of the Tibet Autonomous Region, located at a height of 3663 m in the centre of the Tibetan Plateau (Wang *et al.* 2015). At Darjeeling, a high-altitude location in Eastern Himalayan range the ratio was 0.66 (Chatterjee *et al.* 2010). Pipal and Satsangi (2015) have reported the $PM_{2.5}/PM_{10}$ ratio as 0.66 at Pune, an urban location near Mahabaleshwar. At Sinhagad (1450 m AMSL), another high-altitude site in the Western Ghat mountain range, the ratio was 0.67 (Satsangi *et al.* 2014). The ratio varied for different high-altitude stations due to variation in the concentration of

Table 2. *Mass concentration of PM_{10} and $PM_{2.5}$ and $PM_{2.5}/PM_{10}$ ratios reported from different locations compared with the present study at Mahabaleshwar.*

No.	Site (type)	Altitude (m)	PM_{10} ($\mu g\ m^{-3}$)	$PM_{2.5}$ ($\mu g\ m^{-3}$)	$PM_{2.5}/PM_{10}$	References
1	Lhasa, Tibet (high altitude)	3663	37.7	14	0.37	Wang *et al.* (2015)
2	Sinhagad (high altitude)	1450	35.8	14.1	0.39	Satsangi *et al.* (2014)
3	Darjeeling (high altitude)	2200	29.5	19.6	0.66	Chatterjee *et al.* (2010)
4	Kathmandu, Nepal (high altitude)	1400	169	69	0.41	Putero *et al.* (2015)
5	Pune (urban, metro)	560	139	93	0.67	Pipal and Satsangi (2015)
6	Agra (urban)	171	278	90	0.32	Pipal *et al.* (2011)
7	Mehboobnagar (semi-urban)	450	69	50	0.72	Bisht *et al.* (2015)
8	Delhi (urban, metro)	216	232	118	0.51	Tiwari *et al.* (2015)
9	Lucknow (urban)	123	204	101	0.50	Pandey *et al.* (2012)
10	Patiala (urban)	351	97	57	0.59	Awasthi *et al.* (2011)
11	Lahore (urban)	351	489	91	0.19	Colbeck *et al.* (2011)
12	Beijing (urban, metro)	44	–	86.6	–	Zhao *et al.* (2009)
13	Mahabaleshwar (high altitude)	1348	37.79	26	0.69	Leena *et al.* (2017)
14	Mahabaleshwar (high altitude)	1348	36.93	26.14	0.71	Present study

PM. In this study the average $PM_{2.5}/PM_{10}$ ratio was comparable to or slightly higher than that reported at the above mentioned sites.

3.2 *Seasonal variation of PM*

Seasonal variation of aerosols is determined by changes in source activities, transport from distant sources and changes in meteorological patterns. The season-wise mean concentration of PM_{10} and $PM_{2.5}$ for 2015 to 2016 is shown in figure 4. Analysis of PM data showed that in the year 2015–2016, the mean concentration of PM_{10} in pre-monsoon, monsoon, post-monsoon and winter was 73.5 ± 14.8, 15.6 ± 5.1, 51.6 ± 4.0 and $58.2 \pm 7.3\ \mu g\ m^{-3}$, respectively, whereas that for $PM_{2.5}$ in pre-monsoon, monsoon, post-monsoon and winter was 40.2 ± 6.7, 10.8 ± 2.9, 38.7 ± 1.3 and $43.4 \pm 4.5\ \mu g\ m^{-3}$, respectively. Similarly, in 2016–2017, the mean concentration of PM_{10} in pre-monsoon, monsoon, post-monsoon and winter was 46.0 ± 17.7, 6.8 ± 2.8, 29.6 ± 1.7 and $33.5 \pm 1.8\ \mu g\ m^{-3}$, respectively, whereas that for $PM_{2.5}$ in pre-monsoon, monsoon, post-monsoon and winter was 29.2 ± 8.2, 5.8 ± 2.1, 27.2 ± 1.3 and $30.2 \pm 1.1\ \mu g\ m^{-3}$, respectively. For both the years, the order of observed mass concentration for PM_{10} was pre-monsoon > winter > post-monsoon > monsoon, whereas that for $PM_{2.5}$ was winter > pre-monsoon > post-monsoon > monsoon. High loading of both PM_{10} and $PM_{2.5}$ mass concentrations during the pre-monsoon season is due to the locally generated as well as long-range transported dust (Panicker *et al.* 2013; Tiwari *et al.* 2013), forest fires in nearby forests and an increase in the tourist related activities. The lower concentrations of PM_{10} and $PM_{2.5}$ during the monsoon season are generally associated with the scavenging of aerosols through rain out and wash out processes due to the heavy precipitation received at this site (>5000 mm seasonal mean). A study conducted in a high-altitude research station (5079 m AMSL) by Marinoni *et al.* (2010), recorded the highest aerosol concentrations during the pre-monsoon season that were associated with an increase in anthropogenic activities as well as dry weather conditions. The high concentration of $PM_{2.5}$ in winter could be associated with prevailing meteorological conditions such as low WSs that restrict the dispersion of $PM_{2.5}$ particles and low temperature which is not conducive to the diffusion of $PM_{2.5}$ particles.

3.3 *Diurnal variation of PM*

Besides the daily, monthly and seasonal variability, PM_{10} and $PM_{2.5}$ also exhibit pronounced diurnal variations which are attributed to the local emissions and prevailing meteorology (Dumka *et al.* 2015). The average hourly values of PM_{10} and $PM_{2.5}$ concentrations (figure 5a and b) show significant variations due to the variations in the planetary boundary layer (PBL). Atmospheric conditions also influence certain chemical reactions that lead to the formation of secondary aerosols. The morning peak is mainly attributed to the lifting up of particles due to the breakup of the nocturnal boundary layer by solar heating (Safai *et al.*
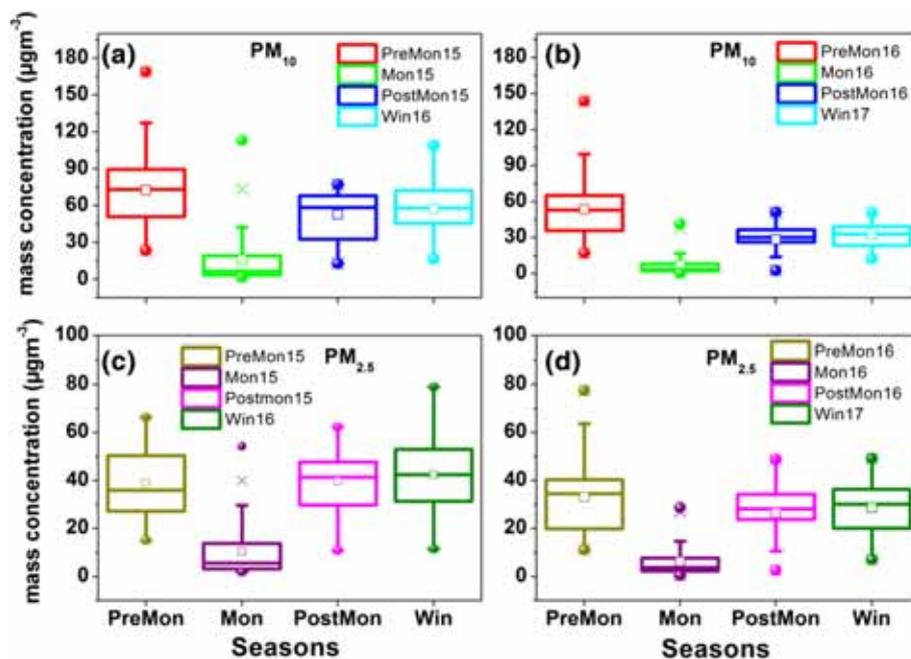
Figure 4. Box and Whisker plots showing seasonal variation of mass concentration of PM_{10} during 2015–2016 (**a**), 2016–2017 (**b**) and that of $PM_{2.5}$ during 2015–2016 (**c**) and 2016–2017 (**d**) over Mahabaleshwar (description: bottom and top of each box represent 25% and 75% quartile, respectively; line inside the box represents median values and small square represents mean, cross represents the outlier, bottom-filled circle represents minimum and upper-filled circle represents maximum values, respectively).

2007). The evening peak could be a combined effect of enhanced traffic emissions due to peak vehicular activity in the evening and the trapping of pollutants as a result of the temperature inversions and lowering of the boundary layer.

Figure 5(a) shows the hourly variation of PM_{10} during different seasons in 2015 and 2016. It is evident from this figure that the concentration of PM_{10} during the pre-monsoon gradually increased after sunrise (6:00 h) and continued up to 16–17 h after which it decreased until succeeding morning. During monsoon, the PM_{10} concentration started to increase after sunrise and peaked at about 12:00 h followed by gradual decrease. During post-monsoon and winter, concentrations of PM_{10} increased gradually from about 06.00 h to peak at around 18–19 h before showing further decrease till next morning but with a small decrease in between 15 and 17 h. However, during the winter season of 2016, the variation of PM_{10} was most uneven with many peaks and lows. Apart from variation in PBL, the effect of the mountain valley winds can influence the observed diurnal variation of PM_{10} in different seasons at Mahabaleshwar. Mountain and valley breezes are local winds caused by geographical feature of the area. During daytime, due to the warming of sun, the air along the mountain slopes raises up creating a valley breeze and carrying pollutants

from valley to the mountain tops. During night hours, the air along the mountain slopes cools and moves down the mountain slopes into the valley, producing a mountain breeze and carrying pollutants from mountain top to the valley. Lang *et al.* (2015) and Bei *et al.* (2018) have reported an impact of mountain valley winds on transport of air pollutants. Interestingly at Mahabaleshwar, concentrations of PM_{10} throughout all the hours were significantly more in 2015 than those in 2016 during post-monsoon and winter. This could be related to higher rainfall in monsoon during 2016 (about 6735 mm seasonal total) than in 2015 (about 3776 mm seasonal total) which might have resulted in scavenging, especially more for coarse particles, i.e., PM_{10}. The ratio values of mean PM_{10} concentration in pre-monsoon, monsoon, post-monsoon and winter in 2015 to those in 2016 were 1.4, 2.2, 1.8 and 1.8, respectively. However, these ratio values for mean $PM_{2.5}$ concentration were 1.2, 1.7, 1.5 and 1.5, respectively, in pre-monsoon, monsoon, post-monsoon and winter.

Hourly variation of $PM_{2.5}$ (figure 5b) showed a continuous increase from 06.00 h with concentrations peaking around 17.00–18.00 h in 2015. A similar pattern was observed during 2016 except a peak at 09.00 h in morning. During monsoon, the concentration of $PM_{2.5}$ showed an increase from
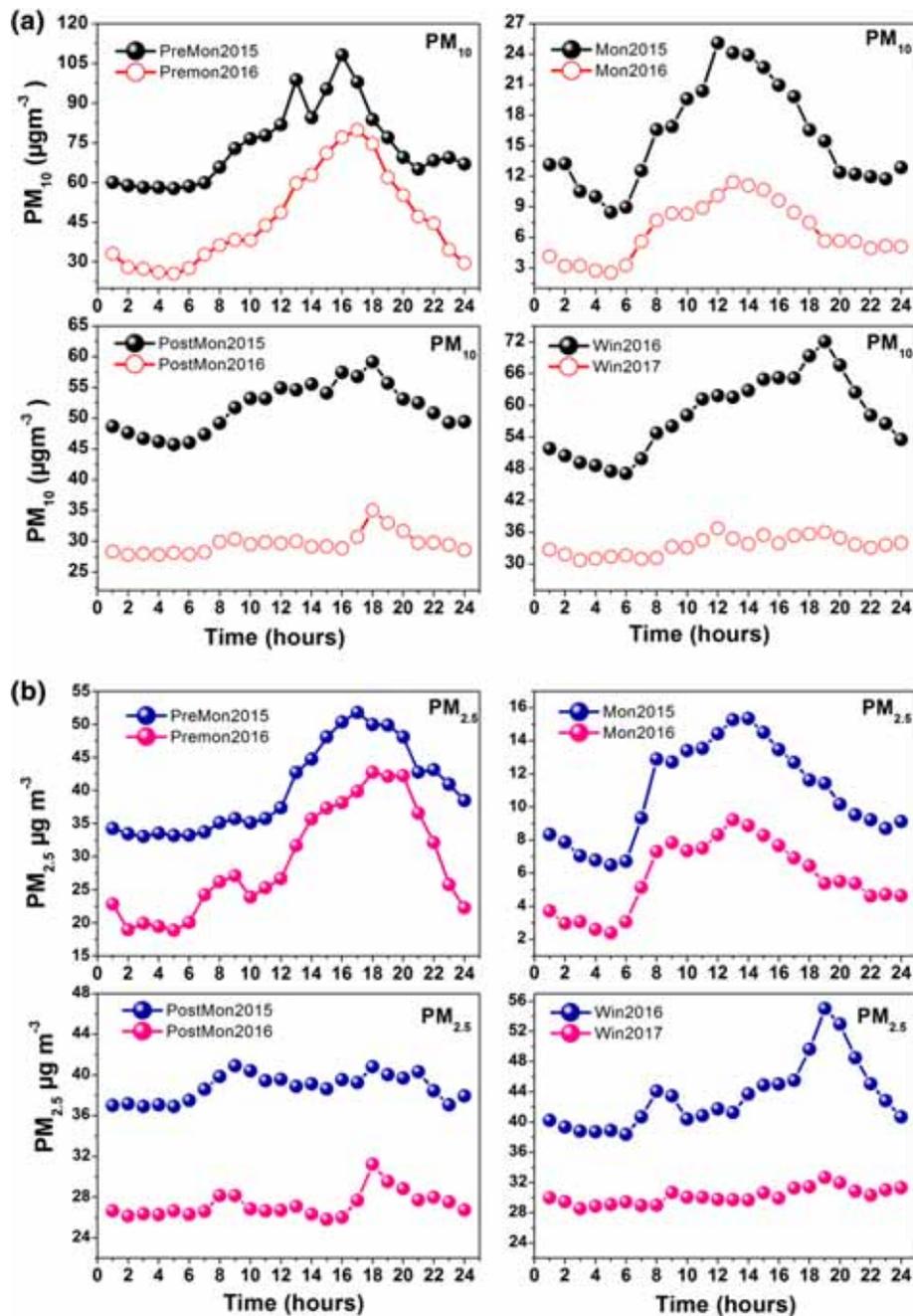
Figure 5. Mean diurnal variation of (**a**) PM$_{10}$ and (**b**) PM$_{2.5}$ concentrations during different seasons in 2015–2016 and 2016–2017 at Mahabaleshwar.

06.00 h in morning which peaked at around 13.00–14.00 h followed by a gradual decrease in 2015 as well as in 2016. Post-monsoon and winter showed similar variation of PM$_{2.5}$ exhibiting bimodal distribution with a morning (08.00–09.00 h) and evening (18.00–19.00 h) peak in 2015 and 2016. The morning and evening peaks coincide with enhanced anthropogenic activities at and near the site, mostly from certain combustion activities (burning of wood, dry leaves and cow dung cakes) for heating purposes in local surroundings (Nair *et al.* 2007). Stull (1988) suggested that the fumigation effect and evolution of the PBL height favour larger aerosol mass concentrations just after the sunrise, which when combined with the rush hour emission results in the higher loading during morning hours. As is observed in the case of PM$_{10}$; the impact of more rainfall during 2016 compared to that in 2015 resulted in high concentration of PM$_{2.5}$ across all the hours during post-monsoon and winter seasons in 2015. Changes in the diurnal pattern during

different years in terms of occurrences of peaks and lows could be related to changes in PBL, mountain valley wind patterns as well as changes in the strength of emission sources in the local surroundings.

3.4 *Air mass back trajectory analysis*

Aerosols over a high-altitude site could be originated either from surrounding local sources or could be transported from other distant sources. At Mahabaleshwar, apart from the vehicular emissions especially from visiting tourist vehicles, certain agriculture related and domestic burning in the close surrounding contributed to the enhancement of PM. However, the possibility of long-range transport from other locations cannot be ruled out. Leena *et al.* (2017) have shown mixing heights reaching even up to 2400 m AGL at Mahabaleshwar. Mixing height depicts the extent of vertical transport from surface sources. Therefore, seven day air mass backward trajectories at a height of 3000 m above the ground level were studied using the HYSPLIT model. This model describes the information on the latitude, longitude and altitude of air mass pathways and is useful to identify the probable source regions (Lelieveld *et al.* 2002; Oanh *et al.* 2016; Ghim *et al.* 2017). Schauer *et al.* (2016) have reported the impact of long-range transport of Saharan dust along with emissions from wildfires over a high-altitude site in Austrian Alps. Figure 6 shows air mass backward trajectory analysis for each season at Mahabaleshwar during the study period. During the pre-monsoon season, air masses appeared to be travelling from the Arabian Peninsula as well as from the Thar Desert in the north western Indian region. In the monsoon season air mass was observed to be from the south west direction, i.e., from over the adjoining Arabian Sea indicating dominance of marine air masses. During post monsoon and winter, the air masses showed transport from the south eastern Indian region as well from the Arabian Peninsula which further passed through northern India. From the air mass back trajectory analysis it can be concluded that aerosols at Mahabaleshwar showed an influence on both marine and continental sources.

3.5 *Meteorological impact on PM*

In addition to the source emission rates, the prevailing meteorology in different seasons plays a key role in determining the fate of aerosols at any given location (Munir *et al.* 2017). Due to the temporal and spatial variation of the pollutant sources in different regions, the characteristics of PM observed in one region cannot be replicated to another region.

Generally, a higher WS is related to lower PM concentrations due to dispersal of particulates. Both $PM_{2.5}$ and PM_{10} showed good anti-correlation with WS across all the seasons indicating dispersal of pollutants due to strong winds at Mahabaleshwar. This is inferred from the negative correlations between $PM_{2.5}$ and WS during monsoon ($r = -0.52$, $p = 0.002$), post-monsoon ($r = -0.48$, $p = 0.01$) and winter ($r = -0.80$, $p < 0.0001$). Similarly, the negative correlation between PM_{10} and WS was observed during monsoon ($r = -0.51$, $p = 0.004$), post-monsoon ($r = -0.75$, $p = 0.001$) and winter ($r = -0.85$, $p = 0.002$). Interestingly, weak or insignificant anti-correlation between WS and both PM_{10} ($r = -0.15$, $p = 0.28$) and $PM_{2.5}$ ($r = -0.12$, $p = 0.45$) was observed during pre-monsoon which can be attributed to the re-suspension of road dust or construction dust caused by enhanced tourist activity. In addition, dust particles carried away by winds from arid regions to the sampling location during this season could be the other reason. He *et al.* (2017) have reported relationship between PM and wind through regional transport at Beijing.

A strong positive correlation was found between atmospheric temperature and PM_{10} in pre-monsoon ($r = 0.87$, $p < 0.0001$), monsoon ($r = 0.90$, $p < 0.0001$), post-monsoon ($r = 0.60$, $p = 0.002$) and winter ($r = 0.69$, $p = 0.001$). Similarly, $PM_{2.5}$ also showed good positive correlation with temperature in pre-monsoon ($r = 0.45$, $p = 0.002$) and monsoon ($r = 0.87$, $p < 0.0001$) and a comparatively less strong positive correlation in post monsoon ($r = 0.25$, $p = 0.03$) and winter ($r = 0.18$, $p = 0.15$). The effect of temperature on the formation of new particles through gas to particle conversion processes is reported by Jallad *et al.* (2013). High temperature promotes the photochemical reaction between precursor gases leading to particle formation (Wang and Ogawa 2015). RH was inversely correlated with PM_{10} ($r = -0.71$, $p = 0.001$) and $PM_{2.5}$ ($r = -0.60$, $p = 0.006$) during monsoon which is attributed to the wet deposition of aerosols. Abundance of atmospheric moisture (RH > 80%) during the monsoon season might have helped fine suspended particles to bind together thereby forming heavier particles which eventually fall down. However, during pre-
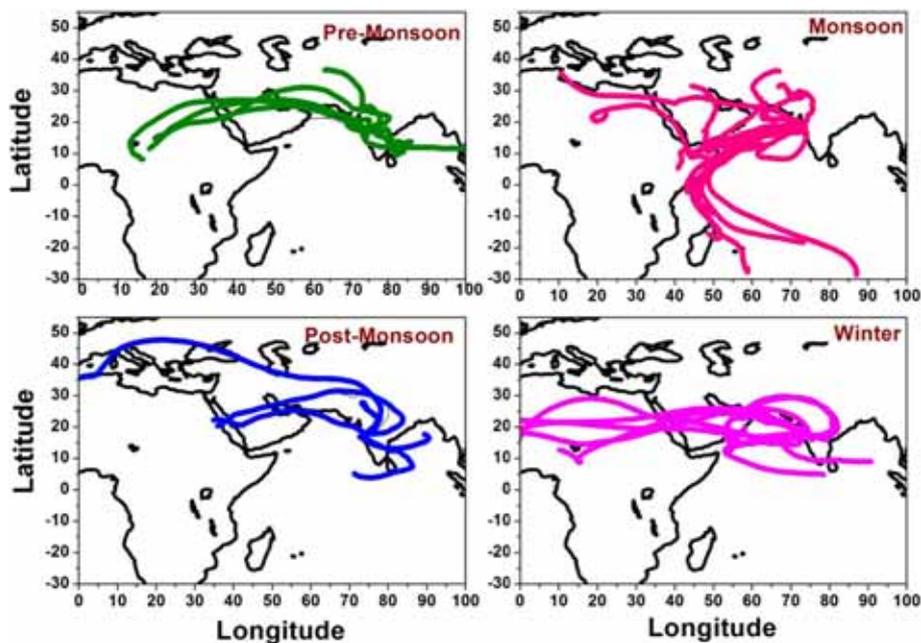
Figure 6. Season wise seven-day air mass backward trajectories at height of 3000 m during different seasons at Mahabaleshwar.

monsoon ($r = 0.38$, $p = 0.01$) and post-monsoon ($r = 0.35$, $p = 0.08$) PM_{10} showed positive correlation with RH indicating moisture related hygroscopic growth of particles. Similarly $PM_{2.5}$ also showed positive correlation with RH in pre-monsoon ($r = 0.78$, $p = 0.002$) and post-monsoon ($r = 0.30$, $p = 0.05$). In contrast, PM_{10} ($r = 0.10$, $p = 0.52$) and $PM_{2.5}$ ($r = 0.04$, $p = 0.75$) did not show a statistically significant correlation with RH during the winter season.

The correlation between PM_{10} and precipitation was negative ($r = -0.53$ and -0.95 in 2015 and 2016, respectively). During the monsoon season, rainfall is responsible for low PM_{10} and $PM_{2.5}$ as they are washed out or scavenged by rain. More than 80% of rainfall over Mahabaleshwar occurs during the monsoon season, leading to strong wet removal of aerosols. The mean seasonal rainfall during monsoon over Mahabaleshwar is >5000 mm. Wet deposition by precipitation or wet removal is one of the main mechanisms for the removal of aerosols from the atmosphere (Jaenicke 1993). The monsoon season is characterised by heavy rain and strong winds both of which are conducive for the decrease in particulate pollutants.

3.6 *Exceedances of threshold limits for PM_{10} and $PM_{2.5}$ levels*

The daily threshold limit set by the CPCB is 60 μg m^{-3} for PM_{10} and 40 μg m^{-3} for $PM_{2.5}$

(CPCB 2009). At Mahabaleshwar, during 2015–2016, the CPCB threshold limit for PM_{10} was exceeded for 43, 04, 30 and 38 days, respectively in pre-monsoon, monsoon, post-monsoon and winter, whereas that for $PM_{2.5}$ was exceeded for 31, 02, 28 and 49 days, respectively, during the same seasons. Comparatively very fewer numbers of exceedances have been observed in 2016–2017. During 2016–2017, the CPCB threshold limit for PM_{10} was exceeded for 21 days in pre-monsoon with no exceedances during monsoon, post-monsoon and winter. Similarly, the CPCB threshold limit for $PM_{2.5}$ was exceeded for 18, 3 and 7 days in pre-monsoon, post-monsoon and winter, respectively, with no exceedances during monsoon (figure 7). Dust content in PM might be an important contributor to the enhanced levels of PM. A satellite and ground-based remote sensing technique is an invaluable tool in studying the long-term variation and transport of dust (Kaufman *et al.* 2005). Ghim *et al.* (2015) have investigated the influence of Asian dust on $PM_{2.5}$ at Seoul. Based on the observations from 14 stations in Seoul, they have reported the occurrences of concentration spikes of $PM_{2.5}$ levels in April and May 2002 when Asian dust storms were the strongest. Apart from the Asian dust effect, prevailing weather conditions were suggested to be conducive to fugitive dust generation during those months. Pu *et al.* (2015) observed enhancement in PM_{10} levels during spring over the Loess Plateau (1965 m AMSL)
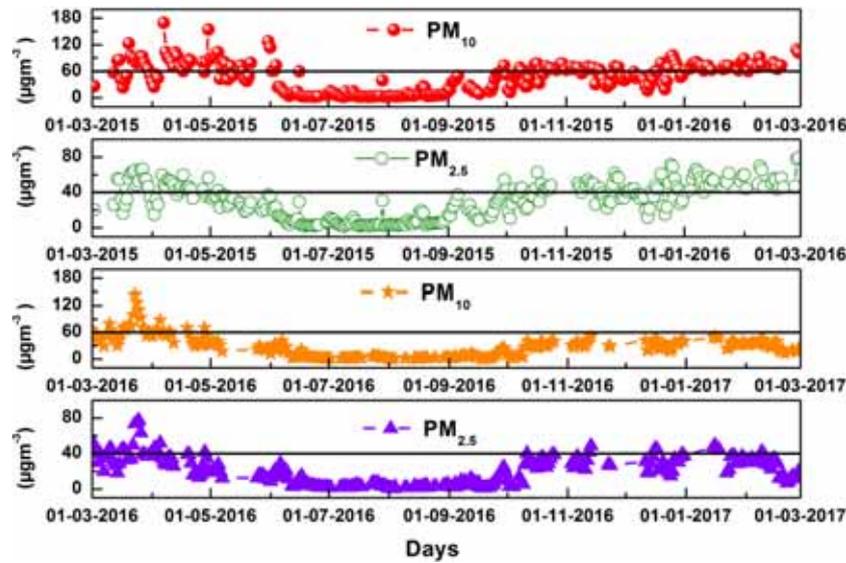
Figure 7. Number of exceedances of CPCB air quality standard values for PM_{10} and $PM_{2.5}$ at Mahabaleshwar.
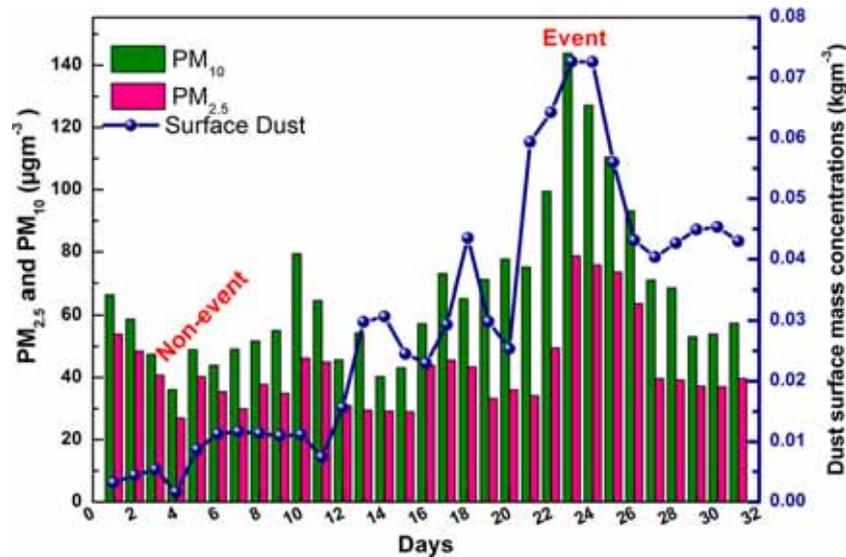

Figure 8. Daily variation of PM_{10} and $PM_{2.5}$ and surface dust concentration obtained from satellite during 1 March to 31 March 2016 over Mahabaleshwar.

which was attributed to the frequent dust events. In India, dust storm events occur frequently over Thar and Margo Desert regions, and influence most parts of the north–north western India during pre-monsoon months from April to June (Pandithurai *et al.* 2008; Srivastava *et al.* 2011). The desert region of North Africa (forming about 65% of the global dust emissions) is the largest source of soil dust suspended in the atmosphere while Asian deserts are the second largest source (25%). Strong dust storm events during pre-monsoon influence the aerosol number size distribution in the accumulation and coarse mode (Dey *et al.* 2004).

We have selected two typical cases representing the day with the highest PM_{10} concentration for 2015 and 2016. On 7th April 2015 the PM_{10} maximum concentration reached 443 µg m^{-3} and $PM_{2.5}$ was 137 µg m^{-3}. Similarly, on 23 March 2016, the maximum concentration was 176.3 and 122.35 µg m^{-3} for PM_{10} and $PM_{2.5}$, respectively. Figure 8 shows the daily variation of PM from 1 March to 31 March 2016. It can be seen that PM values were significantly high on certain days. PM_{10} and $PM_{2.5}$ ground observations over Mahabaleshwar were corroborated with the surface dust mass concentrations (kg m^{-3}) for the month of

(a) Time Averaged Map of Dust Surface Mass Concentration monthly 0.5 x 0.625 deg (kg m⁻³)

(b) mean Daily Omega (Pascal/s)
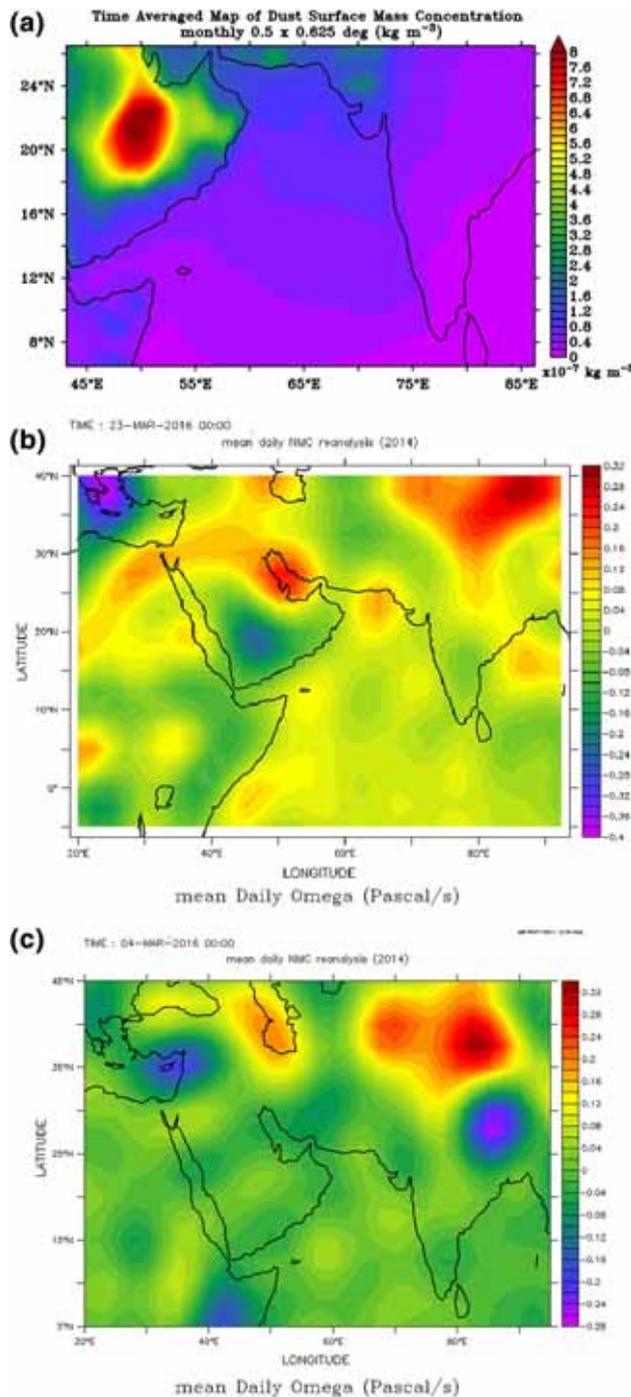
(c) mean Daily Omega (Pascal/s)

Figure 9. (**a**) Surface dust mass concentration in kg m^{-3} for March 2016; (**b**) omega winds at the 1000 hPa synoptic map for 00:00 UTC of 23 March 2016 (dust event) and (**c**) omega winds at the 1000 hPa synoptic map for 00:00 UTC of 4 March 2016 (non-dust event).

March 2016 (figure 9a) obtained from MERRA-2 which is the long term global reanalysis data set to assimilate satellite observations of aerosols representing their interactions with other physical processes in the climate system (https://giovanni.gsfc.nasa.gov/giovanni/, Earth Data, Giovanni,). The

MERRA-2 data matches thoroughly with the PM_{10} and $PM_{2.5}$ ground observations over Mahabaleshwar. It can be seen that the dust surface mass concentration was very low in the first week of March, which gradually increased after 10th March and during 20 to 25 March the dust concentration attained the highest values (0.07–0.08 kg m^{-3}). On 23 March, the highest concentration of PM_{10} and $PM_{2.5}$ was recorded and it can be attributed to dust transported from distant sources.

3.7 *A case study for dust event and non-dust event days*

As stated above, two typical days have been selected on the basis of the mass concentration of PM_{10} and $PM_{2.5}$ as event and non-event days. On 4 March 2016 the PM concentrations were found to be minimum in the month, therefore it is considered as non-event day, whereas, on 23 March the PM concentration was highest and is considered as an event day. Baltaci (2017) has shown the relationship between omega winds and the upward and downward movements of the dust particles. Using this method, the omega winds at the 1000 hPa synoptic map were extracted for 00:00 coordinated universal time (UTC) of March 23. Figure 9(a) shows more dust mass generated over the source region, i.e., Arabian Peninsula during March 2016 and subsequently figure 9(b) and (c) show the mean daily omega wind values (https://www.esrl.noaa.gov/psd/data/gridded/data.ncep.reanalysis.pressure.html) for 23 March 2016 (dust event day) and 4 March 2016 (non-dust event day) which are indicative of the possible extent of downward transport of dust to the observational location. As shown in figure 9(b), sink regions (positive values) owing to the strong downward movements of air are shown indicating possible subsidence of the transported dust in this region leading to enhanced PM. It is quite clear from the spatial plots that there was a transport of dust to the study location on 23 March 2016. However, as seen from figure 9(c), the omega winds at the 1000 hPa synoptic map extracted for 00.00 UTC of 4 March 2016 clearly indicated negative values inferring towards no sink regions indicating no transport of dust to the study location.

We have compared PM_{10} and $PM_{2.5}$ mass concentration, chemical composition of non-refractory submicron aerosols (NR PM_1), meteorological parameters and air mass back trajectories for both event (23 March 2016) and non-event (4 March
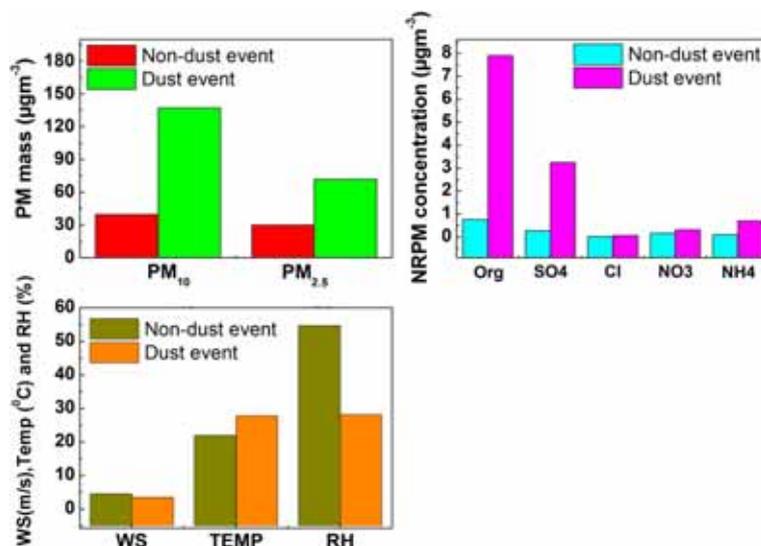
Figure 10. Variation of PM_{10} and $PM_{2.5}$, meteorological parameters and chemical composition of NR PM_1 during non-dust event and dust event days at Mahabaleshwar.

2016) days. The NR PM_1 composition was obtained using ToF-ACSM which is described in section 2. Figure 10 shows the variation of various parameters during non-event and event days. The mass concentration of PM_{10} and $PM_{2.5}$ was significantly higher during the event day as compared to the non-event day. The mean concentration of PM_{10} increased from 39.67 μg m^{-3} on the non-event day to 137.44 μg m^{-3} on the event day. Similarly, the mean concentration of $PM_{2.5}$ increased from 29.90 to 71.94 μg m^{-3}. Zhao *et al.* (2011) reported a significant increase in PM_{10} and $PM_{2.5}$ during dust episodes at the coastal city of Xiamen in China. Among the meteorological parameters, ambient temperature ranged from 23 to 31°C on the event day, whereas on the non-event day, it ranged from 21 to 22°C. The WS was relatively low (1.3 to 1.9 m s^{-1}) on the event day. However on the non-event day the WS varied between 4.3 and 7.4 m s^{-1}. RH was lower on the event day ranging from 15% to 50%, whereas it was 46% to 60% on the non-event day. Since RH was low during dust episodes, it is assumed that the heterogeneous reactions of SO_2 on dust particles could have led to the formation of SO_4^{2-} (Yang *et al.* 2016).

Concentrations of all the observed NR PM_1 components showed higher values on the event day, especially more for organics and sulphate. The mean concentration of organics on the non-event day was 0.76 and 7.9 μg m^{-3} on the event day. Similarly, the mean concentration of sulphate was 0.27 μg m^{-3} on the non-event day and 3.25 μg m^{-3}

on the event day. The main formation pathways of nitrate and sulphate during the dust process are photo-oxidation of NO_2 and SO_2, respectively via OH radicals (Wang *et al.* 2014). The average $PM_{2.5}/PM_{10}$ ratio on the event day was 0.54 and that on the non-event day was 0.69 indicating more coarse-sized dust particles during the dust storm episode. Dust transport from the Arabian Peninsula is one of the important sources which contributed significantly to the PM mass on the dust event day.

As seen from figure 11(a), the air mass back trajectories on an event day 23 March 2016 at 1500, 2500 and 3000 AMSL seem to be coming from the north western region inferring to the impact of long-range transport of dust from the Arabian Peninsula. This is further evident from figure 11(b) which shows a spatial plot of U and V winds over the Indian region on the event day at 850 hPa, showing a cyclonic circulation in the study region and winds approaching from the western dry region (NCEP Reanalysis data at http://www.esrl.noaa.gov/psd/).

Figure 11(c) shows the air mass trajectories for 4 March 2016 (non-event day) at 1500, 2500 and 3000 AMSL. It can be seen that at all the altitudes, the winds are coming from Bay of Bengal passing over the Southern Indian region and then partly over the Arabian Sea before reaching the site. Also, the NCEP spatial plot of U and V winds over the Indian region on 4 March 2016 (non-event day) at 850 hPa (figure 11d) showed majority of the winds from the east-south eastern region.
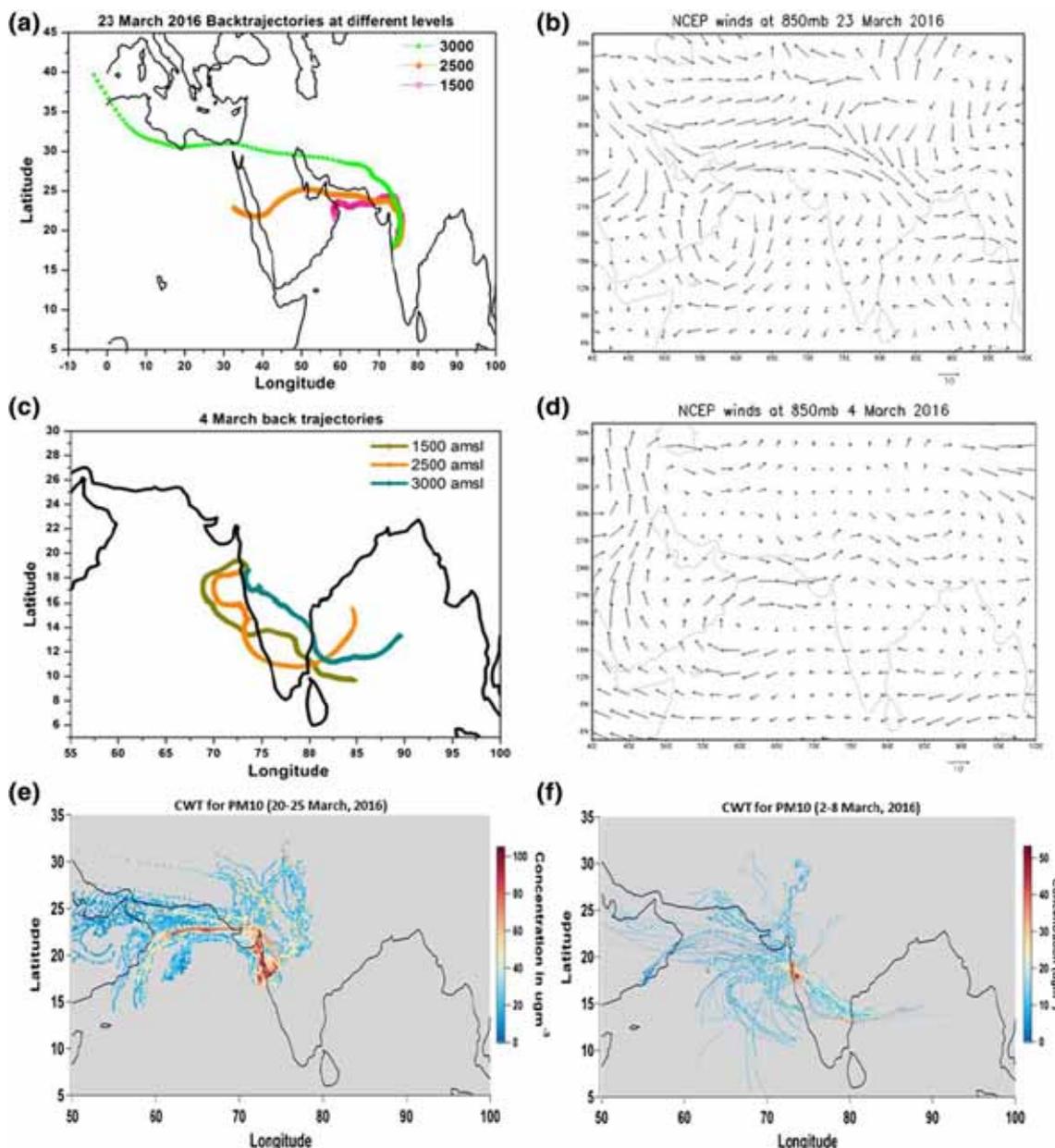
Figure 11. (**a**) and (**c**) show the back trajectories on dust event and non-dust event days at three different altitudes, (**b**) and (**d**) show the spatial plot of U and V winds over the Indian region on an event and non-event days at 850 hPa at Mahabaleshwar. (**e**) CWT for PM_{10} during the event days (20–25 March, 2016) and (**f**) CWT for PM_{10} during non-dust event days (2–8 March, 2016).

To describe the role of transport from other regions, we have performed CWT analysis (Petit *et al.* 2017) on $PM_{2.5}$ and PM_{10} data during the event (20–25 March, 2016) and non-event (2–8 March, 2016) periods. It can be seen from figure 11(e) that during the dust event days, the high concentration of PM is mostly contributed from (i) Gujarat and Thar Desert, (ii) Mumbai Metro City and (ii) African gulf region. The analysis provides evidence for episodes showing an impact of transported dust on observed high concentration of PM. In addition to the long-range dust transport, the possible regional transport from surrounding regions like Gujarat and Mumbai might have contributed significantly to the organics and sulphate mass loading as evident from CWT analysis for event and non-event days. The incursion of certain low-volatile organic vapours and sulphuric acid/sulphur dioxide from these industrial regions could have found more heterogeneous aerosol surface (heterogeneous aerosol processing) to be deposited onto it during dust event days as compared to non-event days. This might have led to the observed higher loading of

organics and sulphate during event days. In contrast to dust event days, the CWT analysis during the non-event days (figure 11f) showed that the PM is mostly contributed by the transport from the Arabian Sea and South Eastern Indian region apart from little contribution from the Mumbai region.

Overall, the current assessment of the fine and coarse particles over Mahabaleshwar will strengthen our understanding about the influence of local sources, long-range transport and local meteorological conditions on the PM over this high-altitude site.

4. Conclusions

Levels of PM_{10} and $PM_{2.5}$ were monitored during March 2015 to February 2017 at Mahabaleshwar, a high-altitude station. The mean concentration of $PM_{2.5}$ was maximum in winter followed by pre-monsoon whereas that for PM_{10} was maximum in pre-monsoon followed by winter. The lowest concentrations for both were observed in monsoon. The winter season experiences more combustion activities in the local surrounding as well as low ventilation of fine particulates due to low-mixing heights thereby showing enhancement in $PM_{2.5}$. The high PM_{10} concentration in the pre-monsoon season was attributed to the long-range transport of dust from the Arabian peninsula, more vehicular emissions due to peak tourist activity and pre-vailing boundary layer conditions. Scavenging of aerosols due to heavy rains at this site resulted in minimum concentrations during the monsoon. The concentrations of $PM_{2.5}$ and PM_{10} were higher in all the seasons in 2015 as compared to 2016 which could be related to comparatively higher rainfall in 2016. The diurnal variation of $PM_{2.5}$ and PM_{10} could be attributed to changes in PBL, mountain valley wind patterns as well as changes in the strength of emission sources in the local sur-roundings. The ratio of $PM_{2.5}/PM_{10}$ suggests the dominance of PM_{10} inferring towards more con-tribution of coarse particles. During the pre-mon-soon season, the concentrations of both $PM_{2.5}$ and PM_{10} exceeded the threshold limit set by CPCB on many occasions which could be attributed to the long-range transport of dust from the Arabian peninsula during dust storm episodes. Chemical species, especially organics and sulphate showed enhancement during dust episodes. Air mass back trajectories and CWT analysis for dust event and non-event days indicated the possible long-range transport of aerosols over the site. The results of the present study inferred to the impact of both local and transported aerosols over a high-altitude location, Mahabaleshwar during the study period.

The present study may have significant climatic implications for this topographically and ecologi-cally very sensitive region over the Western Ghats. The presence of desert dust particles in the atmo-sphere might play a key role in the energy distri-bution and the formation of the regional climate over this high-altitude site.

References

ACES (Department of Environmental Science and Analytical Chemistry), Atmospheric Science Unit, Stockholm University 2012 Equivalence of PM10 instruments at a road traffic site: a study in Stockholm spring 2012, ACES report 4, complied by Areskoug, Hans.

Allan J D, Delia A E, Coe H, Bower K N, Alfarra M, Jimenez J L, Middlebrook A M, Drewnick F, Onasch T B, Cana-garatna M R, Jayne J T and Worsnop D R 2004 A generalised method for the extraction of chemically resolved mass spectra from Aerodyne aerosol mass spectrometer data; *J. Aerosol Sci.* **35** 909–922.

Al Jallad F, Al Katheeri E and Al Omar M 2013 Concentra-tions of particulate matter and their relationships with meteorological variables; *Sustain. Environ. Res.* **23**(**3**) 191–198.

Awasthi A R, Agarwal S K, Mittal N, Singh K and Gupta P K 2011 Study of size and mass distribution of particulate matter due to crop residue burning with seasonal variation in rural area of Punjab, India; *J. Environ. Monit.* **13** 1073–1081.

Baltaci H 2017 Spatial and temporal variation of the extreme Saharan dust event over Turkey in march 2016; *Atmo-sphere (Basel)* **8** 41.

Bei N, Zhao L, Wu J, Li X, Feng T and Li G 2018 Impacts of sea-land and mountain-valley circulations on the air pollu-tion in Beijing–Tianjin–Hebei (BTH): A case study; *Env-iron. Pollut.* **234** 429–438.

Bisht D S, Srivastava A K, Pipal A S, Srivastava M K, Pandey A K, Tiwari S and Pandithurai G 2015 Aerosol character-istics at a rural station in southern peninsular India during

CAIPEEX-IGOC: Physical and chemical properties; *Environ. Sci. Pollut. Res.* **22** 5293–5304.

Burnett R, Pope A, Ezzati M, Olives C, Lim S, Mehta S, Shin H, Singh G, Hubbell B, Brauer M, Anderson H, Smith K, Balmes J, Bruce N, Kan H, Laden F, PrüsseUstün A, Turner M, Gapstur S, Diver W and Cohen A 2014 An integrated risk function for estimating the global burden of disease attributable to ambient fine particulate matter exposure; *Environ. Health Perspect.* **122**(**4**) 307–404.

Carrico C M, Bergin H M, Shrestha A B, Dibb J E and Gomes L 2003 The importance of carbon and mineral dust to seasonal aerosol properties in the Nepal Himalayas; *Atmos. Environ. (UK)* **37** 2811–2824.

CPCB (Central Pollution Control Board), Government of India 2009 Nationalambient air quality standards notification.

Chan C K and Yao X 2008 Air pollution in mega cities in China; *Atmos. Environ.* **42** 1–42.

Chatterjee A, Adak A, Singh A K, Srivastava M K, Ghosh S K and Tiwari S 2010 Aerosol chemistry over a high altitude station at north-eastern Himalayas, India; *PLoS ONE* **5**(**6**) e11122, https://doi.org/10.1371/journal.pone.0011122.

Colbeck I, Nasir Z A, Ahmad S and Ali Z I 2011 Exposure to PM10, PM2.5, PM1 and carbon monoxide on roads in Lahore, Pakistan; *Aerosol Air Qual. Res.* **11** 689–695.

Dey S, Tripathi S N, Singh R P and Holben B N 2004 Influence of dust storms on the aerosol optical properties over the Indo-Gangetic basin; *J. Geophys. Res.* **109** D20211.

Draxler R R and Rolph G D 2003 HYSPLIT (Hybrid Single-particle Lagrangian Integrated Trajectory) Model Access via NOAA ARL READY NOAA Air Resources Laboratory, Silver Spring, MD, http://ready.arl.noaa.gov/HYSPLIT.php.

Du Y, Xu X, Chu M, Guo Y and Wang J 2016 Air particulate matter and cardiovascular disease: The epidemiological, biomedical and clinical evidence; *J. Thorac. Dis.* **8**(**1**) 8–19.

Dumka U C, Kaskaoutis D G, Srivastava M K and Devara P C S 2015 Scattering and absorption properties of near-surface aerosol over Gangetic–Himalayan region: The role of boundary-layer dynamics and long-range transport; *Atmos. Chem. Phys.* **15** 1555–1572.

Frohlich R, Cubison M J, Slowik J G, Bukowiecki N, Prevot A S H, Baltensperger U and Jayne J T 2013 The ToF-ACSM: A portable aerosol chemical speciation monitor with TOFMS detection; *Atmos. Meas. Tech.* **6** 3225–3241.

Gawhane R D, Rao P S P, Budhavant K B, Waghmare V, Meshram D C and Safai P D 2017 Seasonal variation of chemical composition and source apportionment of PM2.5 in Pune, India; *Environ. Sci. Pollut. Res.* **24** 21065–21072.

Ghim Y S, Chang Y and Kim J Y 2015 Temporal and spatial variations in fine and coarse particles in Seoul, Korea; *Aerosol Air Qual. Res.* **15** 842–852.

Ghim Y S, Kim J Y and Chang Y 2017 Concentration variations in particulate matter in Seoul associated with Asian dust and smog episodes; *Aerosol Air Qual. Res.* **17** 3128–3140.

He J, Mao H, Gong S, Yu Y, Wu L, Liu H, Chen Y, Jing B, Ren P and Zou C 2017 Investigation of particulate matter regional transport in Beijing based on numerical simulation; *Aerosol Air Qual. Res.* **17** 1181–1189.

Jaenicke R 1993 Tropospheric aerosols; In: *Aerosol-Cloud–Climate Interactions* (ed.) Hobbs P, Academic Press, San-Diego, CA, pp. 1–31.

Kaufman Y J, Koren I, Remer L A, Tanre D, Ginoux P and Fan S 2005 Dust transport and deposition observed from the terra-moderate resolution imaging spectro radiometer (MODIS) spacecraft over the Atlantic Ocean; *J. Geophys. Res.* **110** 10.

Khemani L T 1989 *Physical and Chemical Characteristics of Atmospheric Aerosols. Air Pollution Control; Encyclopedia of Environmental Control Technology, 2*; Gulf Publ. Co., USA, pp. 401–452.

Lang M N, Gohm A and Wagner JS 2015 The impact of embedded valleys on daytime pollution transport over a mountain range; *Atmos. Chem. Phys.* **15** 11981–11998.

Leena P P, Vijayakumar K, Anilkumar V and Pandithurai G 2017 Analysing temporal variability of particulate matter and possible contributing factors over Mahabaleshwar, a high-altitude station in Western Ghats, India; *J. Atmos. Sol.-Terr. Phys.* **164** 105–115.

Lelieveld J, Berresheim H, Borrmann S, Crutzen P J, Dentener F J, Fischer H, Feichter J, Flatau P J, Heland J, Holzinger R, Korrmann R, Lawrence M G, Levin Z, Markowicz K M, Mihalopoulos N, Minikin A, Ramanathan V, de Reus M, Roelofs G J, Scheeren H A, Sciare J, Schlager H, Schultz M, Siegmund P, Steil B, Stephanou E G, Stier P, Traub M, Warneke C, Williams J and Ziereis H 2002 Global air pollution crossroads over the Mediterranean; *Science* **298** 794–799.

Marinoni A, Cristofanelli P, Laj P, Duchi R, Calzolari F, Decesari S and Bonasoni P 2010 Aerosol mass and black carbon concentrations, a two year record at NCO-P (5079 m, Southern Himalayas); *Atmos. Chem. Phys.* **10**(**17**) 8551–8562.

Munir S, Habeebullah T M, Mohammed Atef M F, Morsy E A, Rehan M and Ali K 2017 Analysing PM2.5 and its association with PM10 and meteorology in the arid climate of Makkah, Saudi Arabia; *Aerosol Air Qual. Res.* **17** 453–464.

Nair V S, Moorthy K K, Alappattu D P, Kunhikrishnan P K, George S, Nair P R, Babu S S, Abish B, Satheesh S K, Tripathi S N, Niranjan K, Madhavan B L, Srikant V, Dutt C B S, Badarinath K V S, Reddy R R 2007 Wintertime aerosol characteristics over the Indo-Gangetic Plain (IGP): Impacts of the local boundary layer processes and long-range transport; *J. Geophys. Res.* **112** D13205.

Ng N L, Herndon S C, Trimborn A, Canagaratna M R, Croteau P L, Onasch T B, Sueper D, Worsnop D R, Zhang Q, Sun Y L and Jayne J T 2011 An aerosol chemical speciation monitor (ACSM) for routine monitoring of the composition and mass concentrations of ambient aerosol; *Aerosol Sci. Technol.* **45** 780–794.

Oanh N T K, Nguyen Hang T, Aungsiri T, Worrarat T and Danutawat T 2016 Characterization of particulate matter measured at remote forest site in relation to local and distant contributing sources; *Aerosol Air Qual. Res.* **16** 2671–2684.

Pandey P, Khan A H, Verma A K, Singh K A, Mathur N, Kisku G C and Barman S C 2012 Seasonal trends of PM2.5 and PM10 in ambient air and their correlation in ambient air of Lucknow city, India; *Bull. Environ. Contam. Toxicol.* **88** 265.

Pandithurai G, Dipu S, Dani K K, Tiwari S, Bisht D S, Devara P C S and Pinker R T 2008 Aerosol radiative forcing during dust events over New Delhi, India; *J. Geophys. Res.*. https://doi.org/10.1029/2008JD009804.

Panicker A S, Lee D I, Kumkar Y V, Kim D, Maki M and Uyeda H 2013 Decadal climatological trends of aerosol optical parameters over three different environments in South Korea; *Int. J. Climatol.* **33** 81909–81916.

Panicker A S, Ali K, Beig G and Yadav S 2015 Characterization of particulate matter and carbonaceous aerosol over two urban environments in Northern India; *Aerosol Air Qual. Res.* **15**(**7**) 2584–2595.

Perez N, Pey J, Querol X, Alastuey A, Lopez J M and Viana M 2008 Partitioning of major and trace components in PM_{10}–$PM_{2.5}$–PM_1 at an urban site in Southern Europe; *Atmos. Environ.* **42** 1677–1691.

Petit J E, Favez O, Albinet A and Canonaco F 2017 A user-friendly tool for comprehensive evaluation of the geographical origins of atmospheric pollution: Wind and trajectory analyses; *Environ. Model. Softw.* **88** 183–187.

Pipal A S and Satsangi P G 2015 Study of carbonaceous species, morphology and sources of fine ($PM_{2.5}$) and coarse (PM_{10}) particles along with their climatic nature in India; *Atmos. Res.* **154** 103–115.

Pipal A S, Kulshrestha A and Taneja A 2011 Characterization and morphological analysis of airborne $PM_{2.5}$ and PM_{10} in Agra located in north central India; *Atmos. Environ.* **21** 3621–3630.

Pu W, Wang X, Zhang X, Ren Y, Shi J-S, Bi J-R and Zhang B-D 2015 Size distribution and optical properties of particulate matter (PM_{10}) and black carbon (BC) during dust storms and local air pollution events across a Loess Plateau site; *Aerosol Air Qual. Res.* **15** 2212–2224.

Putero D, Cristofanelli P, Marinoni A, Adhikary B, Duchi R and Shrestha S D 2015 Seasonal variation of ozone and black carbon observed at Paknajol, an urban site in the Kathmandu Valley, Nepal; *Atmos. Chem. Phys.* **15**(**24**) 13957–13971.

Querol X, Alastuey A and Rodrıguez S 2004 Levels of particulate matter in rural, urban and industrial sites in Spain; *Sci. Total Environ.* **334–345** 359–376.

Rengarajan R, Sudheer A K and Sarin M M 2011 Wintertime PM2.5 and PM10 carbonaceous and inorganic constituents from urban site in western India; *Atmos. Res.* **102**(**4**) 420–431.

Safai P D, Rao P S P, Momin G A, Ali K, Chate D M, Praveen P S and Devara P C S 2005 Variation in the chemistry of aerosols in two different winter seasons at Pune and Sinhagad, India; *Aerosol Air Qual. Res.* **5**(**1**) 115–126.

Safai P D, Kewat S, Praveen P S, Rao P S P, Momin GA, Ali K and Devara P C S 2007 Seasonal variation of black carbon aerosols over a tropical urban city of Pune, India; *Atmos. Environ.* **41** 2699–2709.

Safai P D, Budhavant K B, Rao P S P, Ali K and Sinha A 2010 Source characterization for aerosol constituents and changing roles of calcium and ammonium aerosols in the neutralization of aerosol acidity at a semi-urban site in SW India; *Atmos. Res.* **98** 78–88.

Satsangi P G, Chavan S P, Rao P S P and Safai P D 2014 Chemical characterization of particulate matter at Sinhagad, a high altitude station in Pune, India; *Indian J. Radio Space Phys.* **43** 284–292.

Schauer G, Kasper-Giebl A and Mocnik G 2016 Increased PM concentrations during a combined wildfire and Saharan dust event observed at high-altitude sonnblick observatory, Austria; *Aerosol Air Qual. Res.* **16**(**3**) 542–554.

Singla V, Mukherjee S, Safai P D, Meena G S, Dani K K and Pandithurai G 2017 Role of organic aerosols in CCN activation and closure over a rural background site in Western Ghats, India; *Atmos. Environ.* **158** 148–159.

Song Q, Christiani D, Wang X and Ren J 2014 The global contribution of outdoor air pollution to the incidence, prevalence, mortality and hospital admission for chronic obstructive pulmonary disease: A systematic review and meta-analysis; *Int. J. Environ. Res. Public Health* **11**(**11**) 11822–11832.

Sreekanth V, Mahesh B and Niranjan K 2018 Gradients in $PM_{2.5}$ over India: Five city study; *Urban Clim.* **25** 99–108.

Srivastava A K, Pant P, Hegde P, Singh S, Dumka U C, Naja M, Singh N and Bhavanikumar Y 2011 Influence of South Asian dust storm on aerosol radiative forcing at a high-altitude station in central Himalayas; *Int. J. Remote Sens.* **32**(**22**) 7827–7845.

Stull R B 1988 *An Introduction to Boundary Layer Meteorology*; Kluwer Academic, Dordrecht, pp. 115–149.

Tiwari S, Chate D M, Srivastava M K, Safai P D, Srivastava A K, Bisht D S and Padmanabhamurty B 2012 Statistical evaluation of PM10 and distribution of PM_1, $PM_{2.5}$, and PM_{10} in ambient air due to extreme fireworks episodes (Diwali festivals) in megacity Delhi; *Nat. Hazard* **61**(**2**) 521–531.

Tiwari S, Srivastava A K, Bisht D, Parmita P, Srivastava M K and Attri S 2013 Diurnal and seasonal variations of black carbon and PM 2.5 over New Delhi, India: Influence of meteorology; *Atmos. Res.* **125** 50–62.

Tiwari S, Hopke P K, Pipal A S, Srivastava A K, Bisht D S, Tiwari S, Singh A K, Soni V K and Attri S D 2015 Intra-urban variability of particulate matter (PM2.5 and PM10) and its relationship with optical properties of aerosols over Delhi, India; *Atmos. Res.* **166** 223–232.

van Donkelaar A, Martin R V, Brauer M, Kahn R, Levy R, Verduzco C and Villeneuve P J 2010 Global estimates of ambient fine particulate matter concentrations from satellite-based aerosol optical depth: Development and application; *Environ. Health Perspect.* **118** 847–855.

Wang J and Ogawa S 2015 Effects of meteorological conditions on $PM_{2.5}$ concentrations in Nagasaki, Japan; *Int. J. Environ. Res. Public Health* **12** 9089–9101.

Wang S H, Tsay S C, Lin N H, Hsu N C, Bell S W, Li C, Ji Q, Jeong M J, Hansell R A, Welton E J, Holben B N, Sheu G R, Chu Y C, Chang S C, Liu J J and Chiang W L 2011 First detailed observations of long-range transported dust over the Northern South China Sea; *Atmos. Environ.* **45** 4804–4808.

Wang Y Q, Zhang X Y, Sun J Y, Zhang X C, Che H Z and Li Y 2015 Spatial and temporal variations of the concentrations of PM_{10}, $PM_{2.5}$ and PM_1 in China; *Atmos. Chem. Phys.* **15** 13585–13598.

Wang Y, Zhang Q, Jiang J, Zhou W, Wang B, He K, Duan F, Zhang Q, Philip S and Xie Y 2014 Enhanced sulfate formation during China's severe winter haze episode in January 2013 missing from current models; *J. Geophys. Res. Atmos.* **119** 10425–10440.

Weuve J, Puett R, Schwartz J, Yanosky J, Laden F and Grodstein F 2012 Exposure to particulate air pollution and cognitive decline in older women; *Arch. Intern. Med.* **172**(**3**) 219–227.

WHO 2016 *World Health Statistics 2016*; WHO, Geneva.

Yang T, Sun Y L, Zhang W, Wang Z F and Wang X Q 2016 Chemical characterization of submicron particles during typical air pollution episodes in spring over Beijing; *Atmos. Oceanic Sci. Lett.* **9**(**4**) 255–262.

Zhao J P, Zhang F W, Xu Y, Chen J S, Yin L Q, Shang X S and Xu L L 2011 Chemical characteristics of particulate matter during a heavy dust episode in a coastal city, Xiamen, 2010; *Aerosol Air Qual. Res.* **11** 299–308.

Zhao X, Zhang X, Xu X, Xu J, Meng W and Pu W 2009 Seasonal and diurnal variations of ambient $PM_{2.5}$ concentration in urban and rural environments in Beijing; *Atmos. Environ.* **43** 2893–2900

Corresponding editor: Suresh Babu.